Soft transfemoral prosthetic socket with sensing and augmenting feedback: a case study

Linda Paternò, *Member, IEEE,* Mariangela Filosa, Eugenio Anselmino, Alessio Cecere, Filippo Dell'Agnello, Emanuele Gruppioni, *Member, IEEE,* Alberto Mazzoni, Silvestro Micera, *Fellow, IEEE,* Calogero Oddo, *Senior Member, IEEE,* Arianna Menciassi, *Fellow, IEEE*

Abstract— In lower limb prostheses, the physical interface constituted by the socket is a crucial component for the device success. This work proposes a new design based on a rigid frame integrated into a silicone structure which allows for a more comfortable biomechanical coupling with the residual limb and facilitates the integration of smart technologies. This paves the way for new possibilities for prosthetic bidirectional interfaces or user health monitoring. Thus, four surface EMG sensors, three vibrotactile units, and nine temperature and humidity sensors have been integrated into the socket. These components enable the user's motor intention decoding, provide augmenting feedback, and measure the residual limb thermal condition when wearing the prosthesis.

The new socket was tested on a partecipant with a transfemoral amputation. The sEMG signals were registered during five different tasks in a circuit training and the classification median accuracy of an intention decoding algorithm was found to always be higher than 73%. The user's perception of vibrotactile feedback was assessed through a psychophysical experiment and revealed vibrations from singularly activated units were the best perceived. Questionnaire results confirmed a high satisfaction level. However, tests on temperature and humidity suggest more efforts are still required in terms of skin perspiration.

Index Terms— Augmenting feedback, EMG sensing, prosthetic liner, prosthetic socket, residual limb, transfemoral amputee, volume fluctuations.

I. INTRODUCTION

IN the last few years, various concepts of innovative lower limb prostheses have been developed to mimic the lost biological capabilities and restore the impaired performances of the user, ever more effectively [1]–[3]. In this context, the development of a smart physical human-machine interface becomes essential to seamlessly integrate the prosthesis with the user and advance novel functionalities [4].

In lower limb prostheses, the physical human-machine interface is typically constituted by the socket, a passive rigid structure that replicates the user's residual limb shape to provide a grip on bony prominences and a suction effect on soft tissues [6]. The socket system often includes a soft liner worn on the residual limb before fitting the socket to improve prosthesis comfort and protect the tissues.

The socket system primarily aims to ensure a stable and comfortable biomechanical coupling with the user [5], but the potential to incorporate smart components into it could open up new possibilities in lower limb prostheses. As the socket system serves as the link between the artificial device and biological tissues, integrated smart components could enable a bidirectional interface for a closed control loop of the prosthetic device [12], as well as unobtrusive monitoring of the user's health [13]. Nevertheless, numerous socket-related issues are reported by the majority of lower limb amputees [9], [10]. In particular, current sockets cannot compensate for even small residual limb volume changes, which can occur also in the short term, *e.g.* due to physical activity [9]. This can compromise the fitting and suspension of the socket, hampering the use of the prosthesis. Additionally, lower limb sockets exert high stresses on tissues, leading to various vascular and dermatological complications [5], [10]. The design and materials of the socket and liner also create a physical barrier that affects the user's thermoregulation system, causing sweating and irritation [11]. Due to these issues, embedding sensors and actuators into lower limb sockets proves particularly challenging [5].

Some previous works exploring skin-contact technologies for motion intention decoding or sensory feedback in lower limb prostheses have bypassed the need for a new socket system by placing sensors and actuators outside it, on the proximal healthy part of the residual limb [12]. Nevertheless, these technologies should be seamlessly integrated into the artificial device that the user is already required to use to not compromise the users' acceptance. Additionally, this approach can be applied in transtibial prostheses, but it may be unfeasible in transfemoral ones since the socket covers the entire residual

Linda Paternò, Mariangela Filosa, Eugenio Anselmino, Alessio Cecere, Filippo Dell'Agnello, Alberto Mazzoni, Silvestro Micera, Calogero Oddo, Arianna Menciassi are with The BioRobotics Institute, Sant'Anna School of Advanced Studies, Pisa, Italy, and with Department of Excellence in Robotics & AI, Sant'Anna School of Advanced Studies, Pisa, Italy.

Mariangela Filosa, Silvestro Micera, Calogero Oddo, Arianna Menciassi are with Interdisciplinary Research Center Health Science, Sant'Anna School of Advanced Studies, Pisa, Italy.

Silvestro Micera is with Bertarelli Foundation Chair in Translational Neuroengineering, Center for Neuroprosthetics and Institute of Bioengineering, École Polytechnique Fédérale de Lausanne (EPFL), Lausanne, Switzerland.

Emanuele Gruppioni is with INAIL Centro Protesi, Bologna, Italy.

limb of the user [14]. The main approach reported in the literature for overcoming these challenges is embedding smart components into the liner. Even if this approach has been demonstrated as effective [14]–[19], it strongly limits the exploitable technologies due to the liner design with a few millimeters thickness, its softness, the need to be coupled with the outer socket, and to route component cables out of the liner without hindering the vacuum-based suspension of the prosthesis. Additionally, the liner is worn and removed by rolling it up and down on the residual limb. This daily action can damage the liner and smart components, especially in the case of wired solutions and rigid parts. Soft actuators and sensors could be smoothly integrated, but further advancements are still required to achieve performances comparable to more traditional and robust ones [20]. Another minor aspect is that prosthetic liners do not usually require specific alignment on the residual limb, unlike sockets that enable the alignment of the prosthesis with the user's body. However, some smart components, *e.g.,* surface electromyography (sEMG) sensors,

require specific positions on the residual limb. This additional positioning process of the liner can be particularly complex and time-consuming for the user [14].

Against this background, this work aims to design a new transfemoral soft socket to advance the state-of-the-art in prosthetic physical human-machine interfaces. The proposed socket aims to improve user comfort through a more flexible structure that can passively compensate for small volume changes of the residual limb and lower pressures on the tissues without the need for a standalone liner component. This design facilitates the integration of smart elements into the socket, providing novel solutions for sockets that are not merely passive and rigid structures, but mechatronic devices versatile enough to serve various purposes in the prosthetic field. Thus, sEMG sensors and vibrotactile units have been integrated to demonstrate the potential of using the new socket to enable a bidirectional interface for transfemoral prostheses and temperature and humidity sensors to unobtrusively monitor the residual limb thermal conditions when wearing the prosthesis.
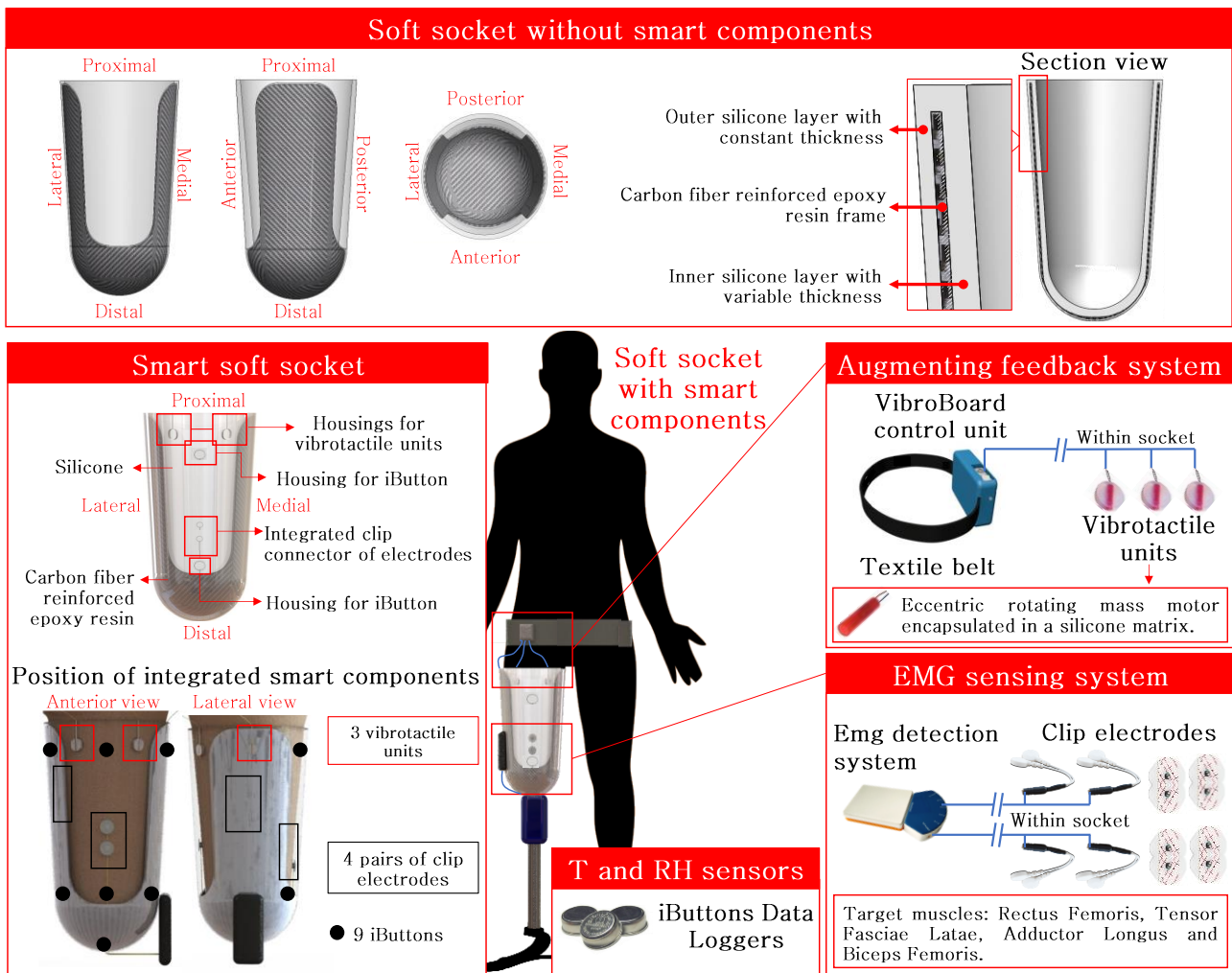

Fig. 1. Design of the soft socket and the integrated technologies. The socket features a flexible frame made of epoxy resin reinforced with carbon fibers embedded in a soft silicone structure. Three vibrotactile units are integrated into the socket in specific housings at the proximal area and in contact with residual limb tissues. They are controlled by a control unit, namely the VibroBoard unit, that the user can wear around the low back thanks to a belt. Four pairs of Ag/AgCl pre-gelled electrodes are integrated in correspondence with the residual limb target muscles and connected to an EMG detection system through mechanical clips integrated into the socket. All the cables are embedded in the soft structure, thus ensuring the vacuum-based suspension system of the socket. Additionally, nine iButtons Data Logger can be positioned in specific housings in the soft structure proximally and distally in the anterior, posterior, lateral, and medial sites, and at the distal end, to monitor the thermal conditions of the residual limb within the socket (RH: Relative Humidity).

II. METHODS

A. Design Overview

The proposed socket consists of a soft silicone structure that integrates a rigid frame of epoxy resin reinforced with carbon fibers (Fig. 1). The rigid structure features a distal hemispheric shape with two parts extended to the proximal area only in the lateral and medial sites. This solution removes a rigid interface in the anterior and posterior regions, thus improving comfort especially in sitting positions. At the same time, it allows for a narrower medio-lateral structure, fundamental for the alignment of the femur with the prosthesis axis, but also for a more flexible prosthetic interface able to compensate for small changes in the volume of the residual limb [5]. Based on the user's preferences and features, the proximal edges of the rigid frame can be featured by a sub-ischial design, *i.e.* with the proximal edge a few centimeters under the ischium [21], or they can create a grip on the great trochanter and on the ischial ramus or tuberosity, as in more traditional Ischial Containment Sockets [22]. The rigid frame is embedded in a soft structure made of 617H43 Silicone Gel (Ottobock). This is constituted by a 5 mm outer layer and an inner layer with a variable thickness increasing from 5 mm proximally to 15 mm distally, thus simulating the shape of commercial prosthetic stand-alone liners, but integrated into the socket itself. This design highly simplifies the integration of skin-contact technologies, since it is composed of a single component instead of a sensorized soft liner that has to be coupled with an outer rigid socket. In this way also prosthesis donning is facilitated. Indeed, the user has to care only about the proper alignment of the socket, as usual, because of the need to align the prosthesis with the body.

The new socket can be worn as traditional solutions with suction suspensions without liners, namely skin-fit sockets (see Fig. 1S in the supplementary material) [5]. In particular, for donning the prosthesis, the user wears a specific low-friction sock with laces on the residual limb. Then, the residual limb is positioned within the socket with the distal end of the sock exiting through the hole of the valve of the suspension system. The sock is then removed by pulling it away through the valve hole, thus pulling the residual limb within the socket.

For the assessment of this new design, an expert prosthetist manufactured a preliminary soft socket without smart elements to quantify its performance in terms of volume compensations. Since the socket is a user-specific component that replicates the residual limb shape, it was designed for a transfemoral residual limb simulator with an embedded fluidic chamber that allows for changing its volume [23]. Subsequently, a transfemoral amputee (TABLE 1) was recruited to manufacture and test a new personalized soft socket integrating the sEMG sensing, augmenting feedback, and temperature and humidity sensors to demonstrate the feasibility of the proposed approach.

B. Volume compensation performances of the soft socket in simulated environment

A 3D scanner (model: GO!SCAN50, Creaform Inc.) was used to measure the initial simulator volume (V_0), which was found equal to 5000 cm^3. Then, the simulator was fixed in position within the new soft socket (Fig. 2, left) and 150 cm^3 of water (ΔV) were supplied to the fluidic chamber at a flow rate of 50 cm^3/min by a syringe pump. This allowed for a simulator volume increment of 3% ($\Delta V / V_0$), which has been found as a characteristic volume fluctuation in the transfemoral amputee population [9]. An F – Socket system (Tekscan Inc.) with two resistive sensors (model: Tekscan Medical Sensor 9833) was positioned on the lateral and medial sites of the simulator / socket interface to measure the pressure changes during the volume increment. This test was repeated five times with the new soft socket (Fig. 2, left) and five times with a more traditional one (Fig. 2, right). In particular, for the traditional one, the Northwestern University Flexible Sub-ischial Vacuum (NU-FlexSIV) Socket was chosen, since reported as the most comfortable and flexible solution in the current state-of-the-art (Fig. 2, right) [21].
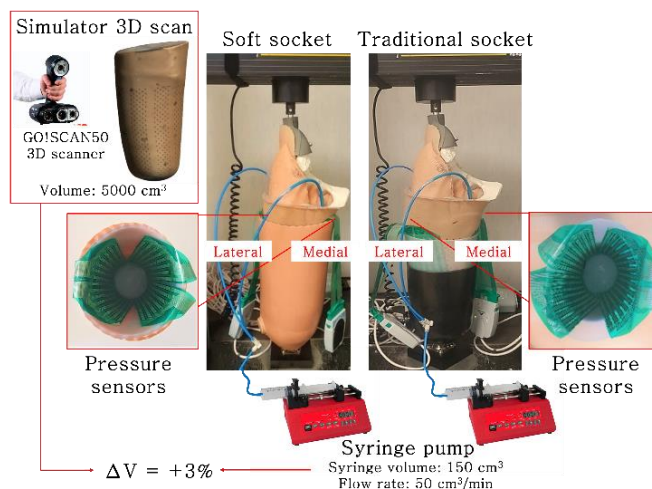

Fig. 2. Experimental set-up for assessing the performances of the new socket (left) in compensating residual limb volume increments with respect to a more traditional design (Northwestern University Flexible Sub-ischial Vacuum Socket, right). Tests were carried out by a residual limb simulator and supplying 150 cm^3 of water in an integrated fluidic chamber which allows for changing its volume. Sensors were positioned at the socket interface to measure pressure changes while increasing the simulator volume.

C. sEMG sensing system

In upper limb prostheses, sEMG signals of residual muscles have become the standard to decode the user's motor intents with a noninvasive approach [1], [8]. This promoted further progress also in socket design and, nowadays, several solutions are available to integrate multiple and different surface electrodes at the prosthetic interface [8], [9]. Although this approach has been demonstrated promising also in lower limb prostheses [10]–[14], only a few studies followed this route [1]. One of the main challenges turns out the integration of smart components into the socket, especially for more proximal amputation levels, such as the transfemoral one [15]–[17], due to the different previously mentioned socket-related issues. Indeed, a robust interface has to be implemented for sEMG recording without hindering the comfort and suspension of the socket itself [18]. In upper limb prostheses, suspension challenges are less pronounced due to lower loads on the socket. In contrast, even minor leakages in the vacuum-based suspension system of the socket can significantly impact the

stability of the prosthesis in lower limb amputees. In this context, the new socket design was exploited to integrate commercial sEMG electrodes in contact with residual limb tissues to test the performances of an intention decoding algorithm.

The sEMG sensing system consisted of four pairs of commercial surface pre-gelled electrodes (model: Ag/AgCl PSG50S) connected to a commercial 64-channel detection device (model: Sessantaquattro, OT Bioelettronica S.r.l.) (Fig. 1). The sEMG signals allowed for the detection of the user's motor intention by the implementation of the algorithm presented in Barberi et al. [29]. The algorithm received as input the Mean Absolute Value (MAV) extracted from the preprocessed sEMG signals of a subfraction of the gait cycle and it outputted the motor task the participant desired to perform. The detectable motor tasks were Ground Level Walking (GLW), Stairs Ascending (SA), Stairs Descending (SD), Ramps Ascending (RA), and Ramps Descending (RD). The classification process exploited a Support Vector Machines based on the Error Correcting Output Code (ECOC) technique.

For decoding the user's motor intentions, the Rectus Femoris, Tensor Fasciae Latae, Adductor Longus, and Biceps Femoris were proved as optimal recording sites in a previous clinical study [26], [29]. Since the position of limb muscles can vary after amputation due to rearrangements during the surgical procedure, the positions of the four electrode pairs were identified by an expert physical therapist and recorded by 3D scanning (Fig. 3a, top). Initially, the physical therapist identified muscles through palpation and then instructed the participant to perform isometric contractions. This facilitated the identification of target muscle positions through contraction and relaxation tasks. Then, the residual limb skin was shaved, an alcohol wipe was used to disinfect and remove sebum, and a slightly damp cloth to prevent excessive skin dryness. The sEMG sensors were positioned and tests were conducted to assess the function of the specific muscles during contraction.
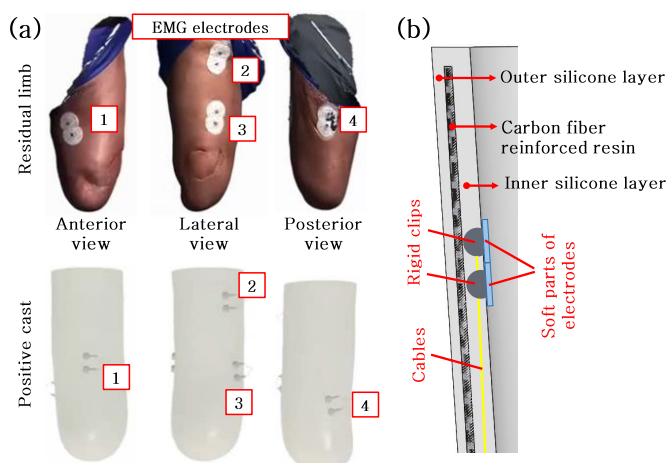

Fig. 3. a) Positioning of the sEMG electrodes on the recruited participant's residual limb (top) and its positive cast (bottom). The electrode pairs 1, 2, 3, and 4 are on the Rectus Femoris, Tensor Fasciae Latae, Adductor Longus, and Biceps Femoris residual muscles, respectively. b) Integration of the electrodes into the socket. The soft parts of the electrodes were not integrated into the socket structure to ensure contact between the electrodes and the tissues, while the rigid clip connectors were within the socket structure to avoid discomfort.

An expert prosthetist made the negative cast of the residual limb with plaster bandages and realized the corresponding positive cast, which was 3D scanned, thus identifying the final positions of the electrode connectors at the prosthetic interface (Fig. 3a, bottom). In the final socket, the soft part of the electrodes is not embedded in the socket structure (Fig. 3b). This can contribute to an increase in pressures applied to the residual limb but should ensure contact between the electrodes and the tissues. In addition, the pressure increment is expected not significant since the soft part of the electrodes is less than 1 mm thick and soft. On the contrary, the rigid clips are embedded in the socket structure and do not exert pressure on the residual limb tissues.

D. Augmenting feedback system

Along with the decoding of the efferent outputs to further control robotic limbs, the restoration of the afferent pathways would be beneficial for gait enhancement. It has been demonstrated that the sensory information coming from the skin, muscles, and joint receptors of the leg has a crucial role in balance and kinematics during locomotion [30], [31]. After an amputation, patients need to learn a new way of decoding such information, mainly relying on the haptic interactions between the residual limb and the prosthetic socket. This requires a high cognitive effort that is usually further exacerbated by limited confidence in using the prosthesis. The high-pressure levels at the socket interface cause several dermatological problems and pain to residual tissues, thus reducing the haptic perception of the residual limb [31], [32]. Furthermore, limb amputees often experience problems related to phantom limb syndrome, which can involve acute or chronic pain, perceptions, and sensations in the absent limb [33]. As a consequence, lower limb amputees usually show gait asymmetries and suboptimal performances when using the prosthesis. Sensory feedback solutions based on vibrotactile technologies have been demonstrated so far to enable improved gait symmetry patterns and postural control [34]–[36]. However, these technologies were always positioned out of the prosthesis, thus affecting the usability of the final device. Thus, a vibrotactile feedback system was embedded into the novel socket to demonstrate the advantages of the proposed solution.

The augmenting feedback system included three VibroTactile (VT) units, each consisting of an eccentric rotating mass (ERM) motor (Pico Vibe 304-116, Precision MicroDrives) encapsulated in a PDMS silicone disk (diameter: 20 mm; thickness 6 mm) for enhancing users' comfort (Fig. 1) [37]. The VT units were controlled by a central unit, namely the *VibroBoard*, through a real-time controller, sbRIO-9651 (National Instruments—NI, Austin, TX, USA), endowed with a Xilinx Zynq-7020 System on Chip. A 667-MHz dual-core ARM Cortex-A9 processor runs a NI real-time operating system and a Field Programmable Gate Array (FPGA) unit Xilinx Artix-7. Each VT unit was driven by a 1 kHz PWM (Pulse-Width Modulation) of a 5V source. The *VibroBoard* unit was housed in a case that can be worn by a belt to not hinder the user's mobility. The VTs were instead embedded into the soft socket, where housings in the proximal area were manufactured on purpose (Fig. 4).

This article has been accepted for publication in IEEE Transactions on Medical Robotics and Bionics. This is the author's version which has not been fully edited and content may change prior to final publication. Citation information: DOI 10.1109/TMRB.2024.3381378

5

> REPLACE THIS LINE WITH YOUR MANUSCRIPT ID NUMBER (DOUBLE-CLICK HERE TO EDIT) <
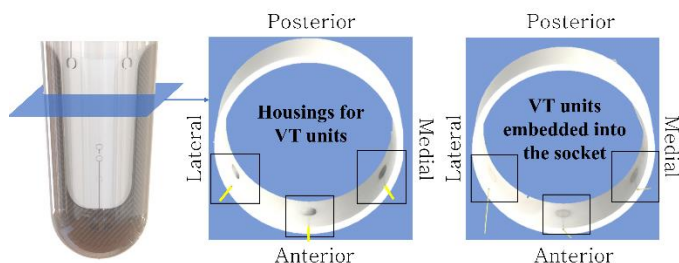

Fig. 4. Positioning of the VibroTactile (VT) units into the socket. The VTs are embedded into the soft socket, where housings in the proximal area were manufactured on purpose by using ad-hoc templates during the socket manufacturing.

Given the strong participant-specific perceptual properties of the residual limb, the positioning of the VTs was previously assessed. In particular, the posterior region was not considered for the delivery of the stimuli, to prevent affecting the user's comfort when sitting. Hence, the lateral, anterior, and medial sides along the circumference of the proximal residual limb were chosen for VT1, VT2, and VT3, respectively. Considering the final configuration of the EMG electrodes and the need to put the VTs far enough from them (at least 2 cm) to prevent affecting the quality of the signals, the final spacing was about 11 cm and 7.5 cm between VT1 and VT2 and between VT2 and VT3, respectively.

E. Thermal conditions of the residual limb within the socket

Nine commercial Hygrochron Data Logger iButtons (Maxim Integrated Products Inc – USA; model: DS1923-F5#; 11-bit resolution: 0.0625 °C for temperature and 0.04% for relative humidity; sampling time: 5 s) [38] were also temporarily integrated into the socket after having been calibrated by a climatic chamber [18]. The iButtons allowed for measuring both temperature and relative humidity of the residual limb skin within the socket. In particular, they were positioned into specific housings manufactured at the socket interface proximally and distally in the anterior, posterior, lateral, and medial sites, and at the distal end (see Fig. 6). After the thermal characterization, the iButtons were removed and the housings were filled with silicone gel buttons to recreate a smooth interface.

F. Human participant tests

The general features of the recruited transfemoral amputee are reported in TABLE 1. The design study was approved by the Joint Ethical Committee of the Scuola Superiore Sant'Anna and Scuola Normale Superiore (Approval no. 11/2021) and the tests were carried out at the prosthetic center Franchi Ortopedia (Cascina, PI, Italy). All experiments were undertaken in accordance with the World Medical Association's Code of Ethics and the Declaration of Helsinki. The recruited participant signed an informed consent form to take part in the test sessions.

During tests, the participant was asked to perform a circuit training, at his usual speed in daily life, including the five different locomotion tasks that the motion intention decoding algorithm could infer (i.e., GLW, SA, SD, RA, and RD, Fig. 5). This circuit training was repeated 15 times with a 5-minute break in between to avoid the participant's fatigue. During

trials, the gait events were identified using signals of a footswitch placed under the participant's foot. At the beginning and end of the experimental session and between the two trials, the sEMG signals were recorded during four muscle contractions in a standing position to perform a further Signal-to-Noise Ratio (SNR) analysis.

TABLE 1
PARTICIPANT'S GENERAL FEATURES

Sex	Man
Age	50 years old
Weight	88 kg
Time since amputation	32 years
Amputation cause	Traumatic event
Own socket design	Ischial Cointainment Socket of carbon fiber reinforced epoxy resin without liner
Suspension system	Passive vacuum suspension based on unidirectional valve
Activity level	K3*

*K level: rating system used to indicate the individual's potential functional ability. K1: no ability to ambulate; K2: able to perform activities typical of limited community ambulatory; K3: able to perform activities typical of community ambulatory; K4: able to perform high-impact activities.
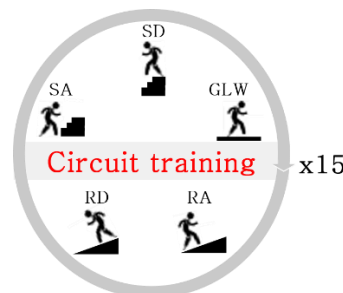

Fig. 5. Experimental protocol for recording sEMG signals. The protocol was featured by a circuit training including five different tasks (Ground Level Walking (GLW), Ramps Ascending (RA), Ramps Descending (RD), Stairs Ascending (SA), Stairs Descending (SD)). It was repeated for 15 times with a 5-minute break in between.

For the post-processing of the acquired data, three representative subwindows of the gait cycle were selected to test the efficacy of the algorithm presented in Barberi et al. [29]. Each subwindow provided the classification output at a different percentage of the ongoing step. The first one considered the EMG signals acquired between 0% and 100% of the gait cycle, the second between 0% and 60%, and the third between -30% and 20%. In the latter case, the intention decoding algorithm used the last portion of the previous gait cycle. Each window was tested by performing a 5-fold cross-validation on the acquired dataset, after the implementation of the preprocessing and feature extraction pipeline described in Section II-C. The tests were repeated with two different Support Vector Machines kernels (linear and 2nd-order polynomial) to show the algorithm behavior when using approaches that present different computational loads.

The appropriate integration of the augmenting feedback device into the socket was assessed through a psychophysical experiment. Specifically, the recruited participant was asked to localize random stimuli delivered over the residual limb surface while wearing the socket in either the sitting or standing position. After a familiarization session, where the

experimenter provided the participant with known vibration events, five experimental trials were performed. The activations of one, two, three, or no VT units at three different intensities (i.e., 50%, 70%, and 100% PWM, corresponding to an ERM motor acceleration peak of about 2g, 3g, and 4g, respectively) were repeated four times per trial, having 96 stimuli each and 480 stimuli overall during the experiment. To avoid expectation effects, the delivery of the stimuli was randomized across the trials. At each event, the participant was asked to identify the vibrating units and the experimenter recorded the answers on a dedicated LabVIEW (National Instruments Corp) GUI (Graphical User Interface). A 5-minute rest period between consecutive trials was taken to avoid the participant's fatigue. The collected data were analyzed in MATLAB (Mathworks, Inc) to assess the participant's accuracy in localizing the stimuli, computed as the number of the right answers over the total amount of the delivered feedback events per each intensity level. The normalized confusion matrices for both postures were also extrapolated to identify the misclassification among all the activation conditions for all the stimulation levels grouped together.

Finally, the intra-socket temperature and relative humidity were collected by the nine iButtons during 30 minutes of resting, 20 minutes of briskly walking at a self-selected speed (~ 6 km/h) on a treadmill (to examine the thermal conditions of the residual limb in a worst-case scenario of high fatigue), and 30 minutes of resting post-exercise (Fig. 6). The mean and standard deviation of nine sensors were evaluated on the initial and final 1-minute recorded data of the two resting periods.

Upon the completion of all tests, the participant was asked to fill out the Socket Comfort Score (SCS) [39] and a modified Prosthetic Evaluation Questionnaire (PEQ) focused on the comfort and fitting of the prosthetic socket [40], [41].
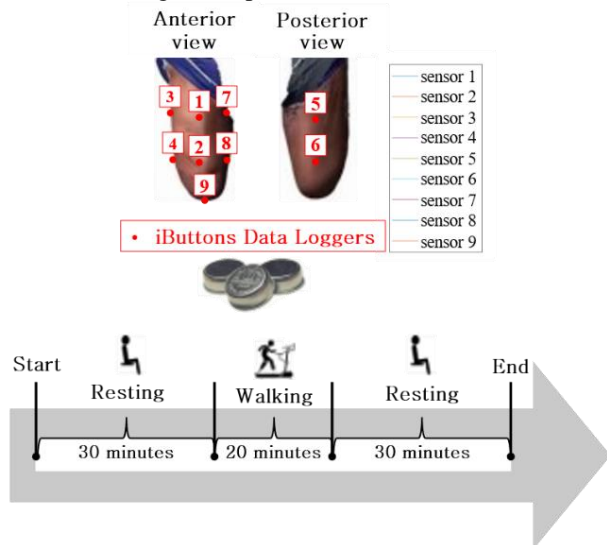

Fig. 6. Positioning of the iButtons Data Loggers integrated into the socket inner surface in contact with the residual limb and experimental protocol for assessing the temperature and relative humidity within the socket.

G. Manufacturing

The manufacturing of the soft socket started with the development of the rigid frame when the positive cast of the residual limb was done (Fig. 3a).
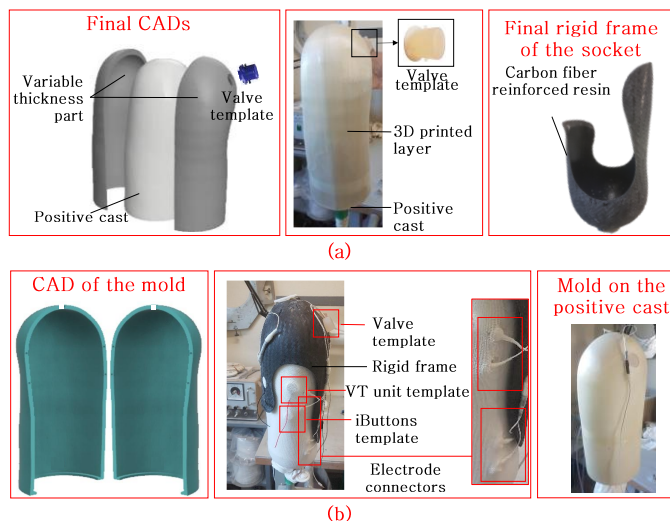

Fig. 7. (a) Manufacturing of rigid frame: a variable thickness part was designed and 3D printed to be positioned on the positive cast. Then, the rigid frame was manufactured by co-infusion technique. **(b)** Manufacturing of soft structure: a specific mold was designed and positioned on the positive cast with the rigid frame, electrode connectors, and the templates of the valve, VT units, and iButtons. Hence, silicone gel was poured into the mold.

In particular, a CAD of the inner variable thickness silicone layer of the socket was designed in SolidWorks starting from the 3D scan of the positive cast (Fig. 7a). It was 3D printed in PLA material together with a valve template required for the integration of the suspension system based on a unidirectional valve (21Y14, Ottobock) at the lateral-distal area of the socket [5]. These components were positioned on the residual limb positive cast and the rigid frame of carbon fiber reinforced epoxy resin was manufactured by lamination technique.

Similarly, a specific mold for the socket soft structure and the templates of the VT units and iButtons were developed (Fig. 7b). The 3D printed variable thickness part was removed and the templates, rigid frame, and electrode connectors were fixed on the positive cast and subsequently closed within the 3D printed mold. Afterward, the soft structure was manufactured by injecting silicone gel within the mold.

When the silicone gel was polymerized, the external silicone layer on the rigid frame was cut to minimize the weight of the final socket, and an aesthetic sock was glued to the external surface. The final soft socket, with a total weight of 1.8 kg, is shown in Fig. 8.
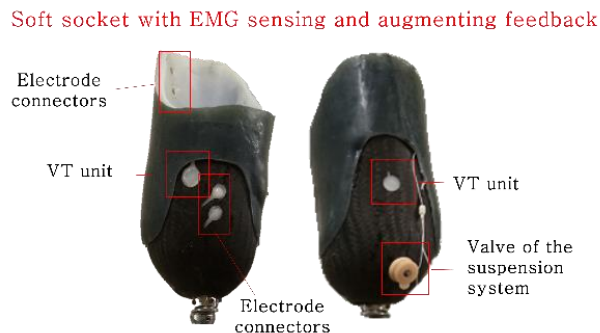

Fig. 8. Final soft socket with four sEMG sensors and three vibrotactile (VT) units (medial view, left; lateral view, right).

III. RESULTS

A. Volume change compensation performances

The pressure changes measured at the socket interface due to the simulator volume increment of 3% are reported in Fig. 9, for both the new soft socket and the more traditional NU-FlexSIV one. For all sensors, the pressure remains approximately constant until a volume increment of 25 cm^3 (i.e., +0.5% volume change) and subsequently increases linearly. In both designs, higher values were measured at the medial side than the lateral one. At a volume increment of 150 cm^3 (+3%), the pressure difference between the medial and lateral areas was 13.8 kPa for the soft socket and 10.96 kPa for the NU-FlexSIV Socket. This is probably related to the traditional shape of transfemoral sockets that apply higher pressures on the medial region, especially at the proximal level, near the ischial tuberosity and the Scarpa's triangle [5].
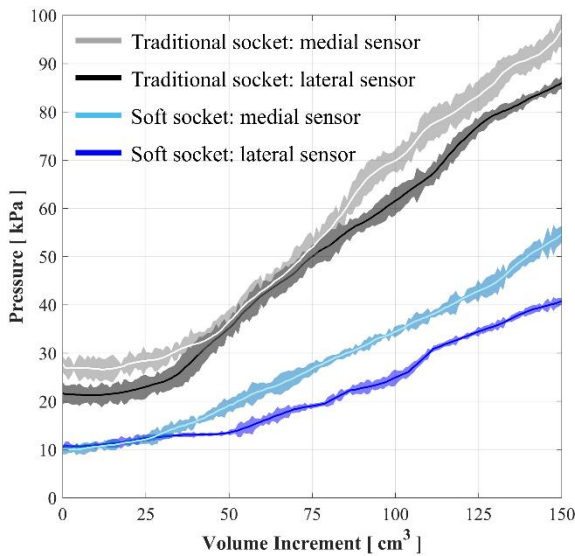

Fig. 9. Mean and standard deviation of the pressure changes at the medial and lateral sites of the socket interface while the volume of the residual limb simulator was increased by 3% (corresponding to an increment of 150 cm^3). The experimental test was carried out five times with a soft socket and five times with a more traditional NU-FlexSIV Socket (see Fig. 2).

As expected, the soft socket was able to compensate for the volume changes in a more efficient way. In particular, when the volume was increased of 150 cm^3 (+3%), the pressure was lower of 42.3 kPa (medial sensor) and 44.8 kPa (lateral sensor) for the soft socket with respect to the NU-FlexSIV Socket. Furthermore, the volume change caused a pressure increment of 66.4 kPa laterally and 71.5 kPa medially in the NU-FlexSIV Socket, versus 31.2 kPa laterally and 45.3 kPa medially in the new soft socket.

B. EMG sensing system

The sEMG signals acquired by the smart socket were found stable and suitable for the implementation of intention detection algorithms. The signals acquired during static contractions tests turned out visible for all the channels except for the Biceps Femoris one (Fig. 10) and their SNR remained stable across the experimental session, both before, during, and after the execution of the locomotion tasks (TABLE 2).
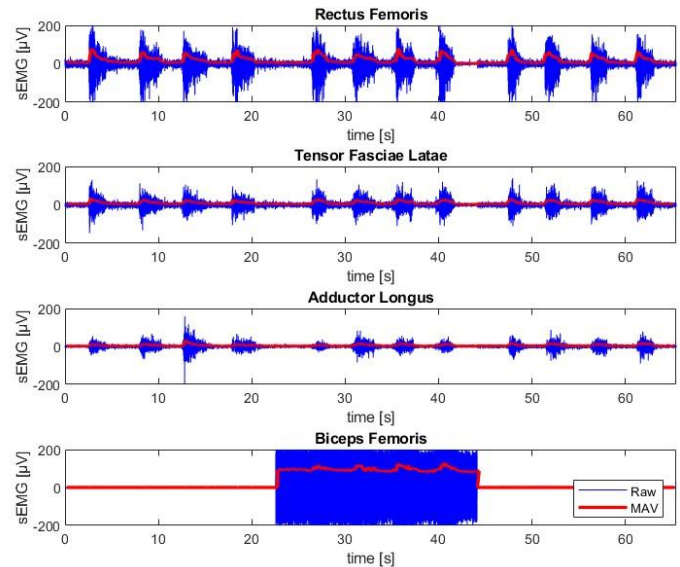

Fig. 10. Plot of the preprocessed sEMG signals and the MAV of the static contraction tests. The first acquisition has been performed before the execution of the locomotion tasks, the second between the two acquisition trials, and the third at the end of the experimental session.

The lower SNR of the Bicep Femoris channel was probably due to damage to the corresponding electrode during the insertion of the residual limb into the socket. Indeed, Ag/AgCl pre-gelled electrodes present an adhesive surface to ensure stable contact with the skin, and this adhesive surface may have been damaged during the socket donning. As shown in Fig. 11, the median accuracy across the folds was higher than 73% for both the linear and polynomial kernels cases but tended to decrease when using the [-30%, 20%] acquisition window. Despite the similarities in terms of accuracy, the interquartile range (IQR) was found to be lower for the polynomial kernel version of the algorithm, indicating an increase in performance stability.

TABLE 2
SIGNAL-TO-NOISE RATIO DURING STATIC CONTRACTION TESTS [dB]

	Rectus Femoris	Tensor Fasciae Latae	Adductor Longus	Biceps Femoris
Acquisition 1	13.22	9.92	12.05	0.55
Acquisition 2	13.79	10.92	10.21	1.11
Acquisition 3	15.11	11.07	10.48	1.20
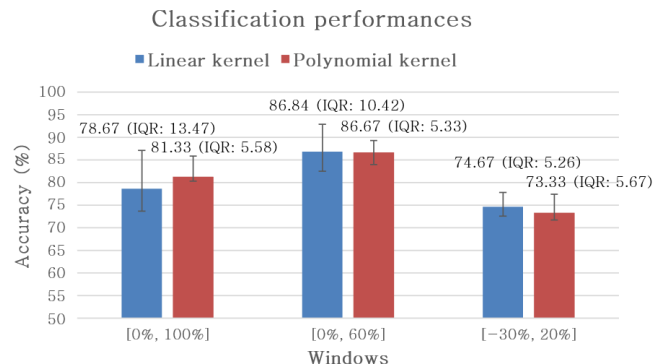
Fig. 11. Performances of the classification algorithm expressed as median and IQR across the folds.

C. Augmenting feedback system

The participant's accuracy in identifying the vibrotactile stimuli is represented in Fig. 12. In particular, the at each VT activation level (2g, 3g and 4g) and the combination of all of them are shown across the five trials (median, (25th percentile, 75th percentile)) for both the sitting and the standing positions. The accuracy was 71.88% (69.53%, 75.78%) at 2g, 75% (70.84%, 81.25%) at 3g, 81.25% (73.44%, 90.63%) at 4g and 76% (70.23%, 82.55%) grouping all the stimulation levels together in the sitting position. For the standing position, the accuracy was 65.63% (57.81%, 72.66%) at 2g, 78.13% (71.10%, 85.16%) at 3g, 75% (75%, 81.25%) at 4g and 73.95% (69.53%, 76.30%) grouping all the stimulation levels together. In addition, the outcomes collected through the LabVIEW GUI were elaborated in MATLAB to evaluate the normalized confusion matrices reported in Fig. 12 and in Fig.2S of the Supplementary Material. The normalized confusion matrices illustrate the percentage of classification accuracy at each VT activation condition (Fig. 12, right) and at each stimulation intensity level (Fig.2S).

D. Intra-socket temperature and humidity and user's satisfaction

Fig. 13 shows the temperature and relative humidity during 30 minutes of resting, 20 minutes of walking, and 30 minutes of resting after physical activity. The mean and standard deviation of the nine sensors on the initial and final 1-minute recorded data of the two resting periods are reported in Fig. 13. While the relative humidity increased continuously throughout the data collection period, the temperature values were more variable. Particularly, they highly increased during the initial 15 minutes of the 1st resting period and with the beginning of the physical activity. During the 2nd resting period, a reduction of the temperature occurred but without reaching the before exercise values.

The Socket Comfort Score was found equal to 8/10 for the recruited amputee, thus confirming the overall comfort of the new solution. The results of the modified PEQ confirmed a high satisfaction level, with no value rated lower than 7/10.
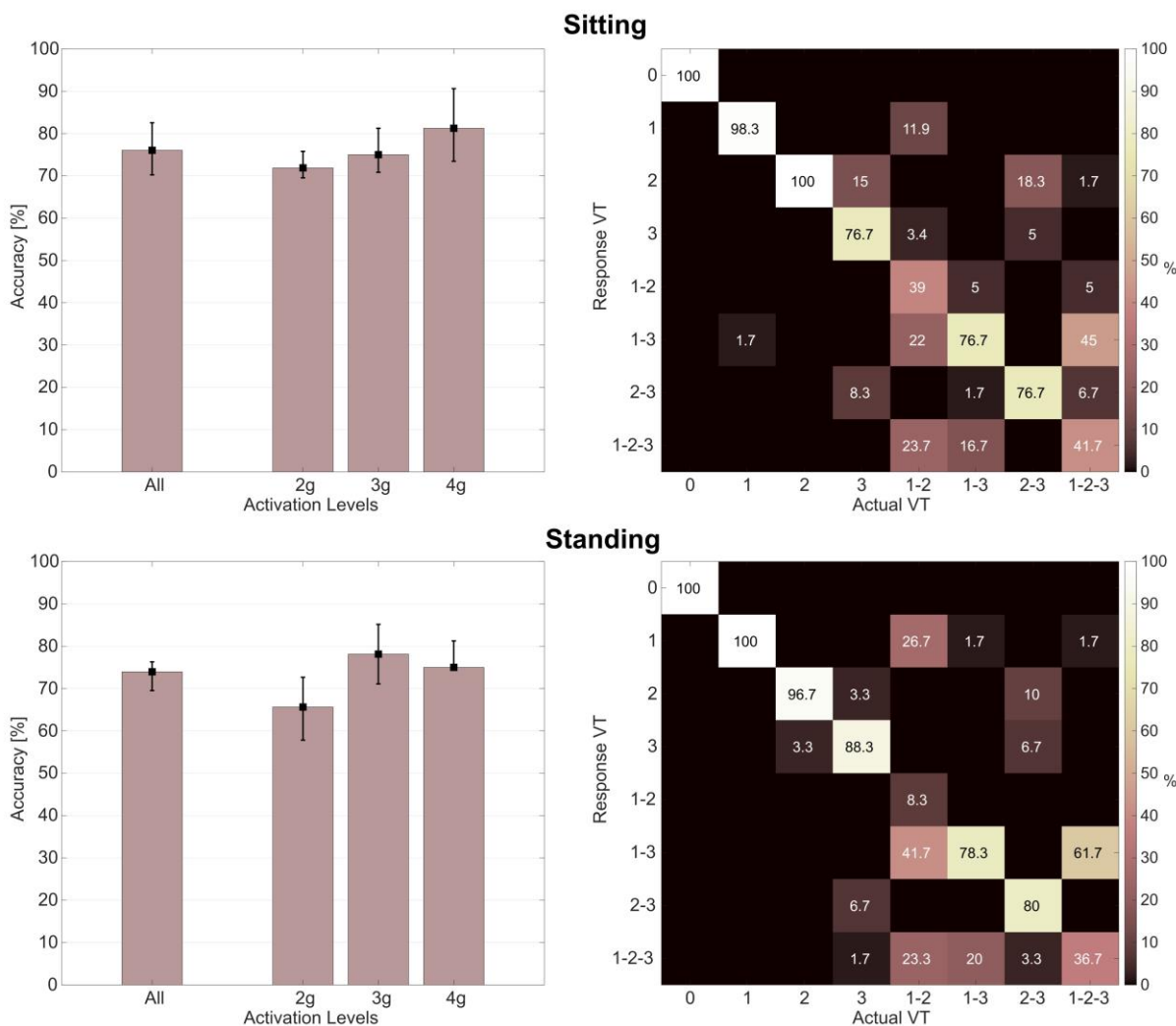

Fig. 12. Results of the psychophysical experiment to assess the feasibility of integrating the sensory feedback device into the socket. Both the sitting (top) and the standing (bottom) position analyses are reported. On the left: the accuracy (median and interquartile range values) to perceive and identify the activated VT is reported at each activation level across the 5 trials. The overall performance (All activation level case) is reported as well. On the right: normalized confusion matrix to investigate the localization ability of the recruited participant when considering the activation of single VTs, pairs and triple of VTs. All the stimulation levels are grouped together.

TABLE 3
INTRA-SOCKET TEMPERATURE AND RELATIVE HUMIDITY

	T [°C]	RH [%]
Start of 1st resting period	28.7 ± 2.5	65.1 ± 4.0
End of 1st resting period	29.8 ± 2.8	75.3 ± 5.9
Start of 2nd resting period	31.1 ± 2.5	80.6 ± 8.8
End of 2nd resting period	31.0 ± 2.4	85.5 ± 9.5

Mean and standard deviation of the data recorded during the initial and final minute of the two resting periods, before and after physical activity. RH: Relative Humidity.

IV. DISCUSSIONS AND CONCLUSIONS

A closed human-centered control loop in robotic lower limb prostheses is essential for yielding the device as an integral part of the user's body. To this end, the prosthetic socket, which represents the physical interface of limb prostheses, should integrate sensors and actuators to allow for a bidirectional interface for decoding the user's motion intention and returning augmenting feedback. Additionally, for persons with limb loss, the prosthesis provides an ideal solution for integrating sensing technologies to monitor the user's health with a non-intrusive approach. Nevertheless, integrating smart technologies in wearable physical interfaces is still an open challenge, particularly in lower limb prostheses due to the different parameters affecting the socket comfort [5].

In this study, a new socket design has been proposed in order to overcome some limitations of previous solutions and simplify the integration of sensors and actuators in contact with the user's residual tissues. The socket features a quite flexible structure that allows for compensating more effectively volume increments which can affect the residual limb over time. Indeed, by using a variable volume simulator of a transfemoral residual limb, the pressure changes due to a volume increment of 3% were verified with the new socket and an existing one (i.e., the NU-FlexSIV Socket). Pressure results were found equal at 41.2 kPa and 54.6 kPa at the lateral and medial sides in the new socket versus 86.0 kPa and 96.9 kPa in the other one (Fig. 9).

Even if the shape of the NU-FlexSIV Socket generally applies higher pressures due to its specific design [10] – as can be noted by the higher initial pressure values of the NU-FlexSIV Socket in Fig. 9 – the pressure change due to the 3% volume increment was found equal to +66.4 kPa laterally and +71.5 kPa medially in the NU-FlexSIV Socket, versus +31.2 kPa laterally and +45.3 kPa medially in the new soft socket. Volume increases within a day in the transfemoral amputee population have been found +2.6% due to prosthesis removal and +3.2% due to physical activity [9]. Thus, the proposed socket turns out a possible solution to achieve a prosthetic physical interface able to adapt to the residual limb volume changes in the short term, more effectively with respect to other designs and without the need of integrating bulky and heavy actuation systems [42].

To demonstrate the feasibility of the proposed approach to allow for a bidirectional interface exploitable in robotic lower limb prostheses, a transfemoral amputee was recruited and a new socket with integrated sEMG sensing and augmenting feedback was developed. In addition, nine iButtons have been integrated temporarily within the socket to assess the thermal conditions of the residual limb. In the future, they could be integrated into the final prototypes during specific time slots, for example, during medical controls, to monitor the thermal conditions at various intervals. Indeed, iButtons can collect a limited amount of data and store it in integrated memory. If different types of sensors are selected, they could be permanently integrated into the socket to enable early detection and prevention of patient deterioration. This solution has the potential to overcome the patients' current self-monitoring approach. Indeed, self-monitoring often triggers clinical actions too late, when symptoms are visible but too severe for effective non-invasive treatment. Therefore, a proactive healthcare system capable of enabling sudden detections is of crucial importance, and the proposed socket design paves the way for future advancements in this direction.
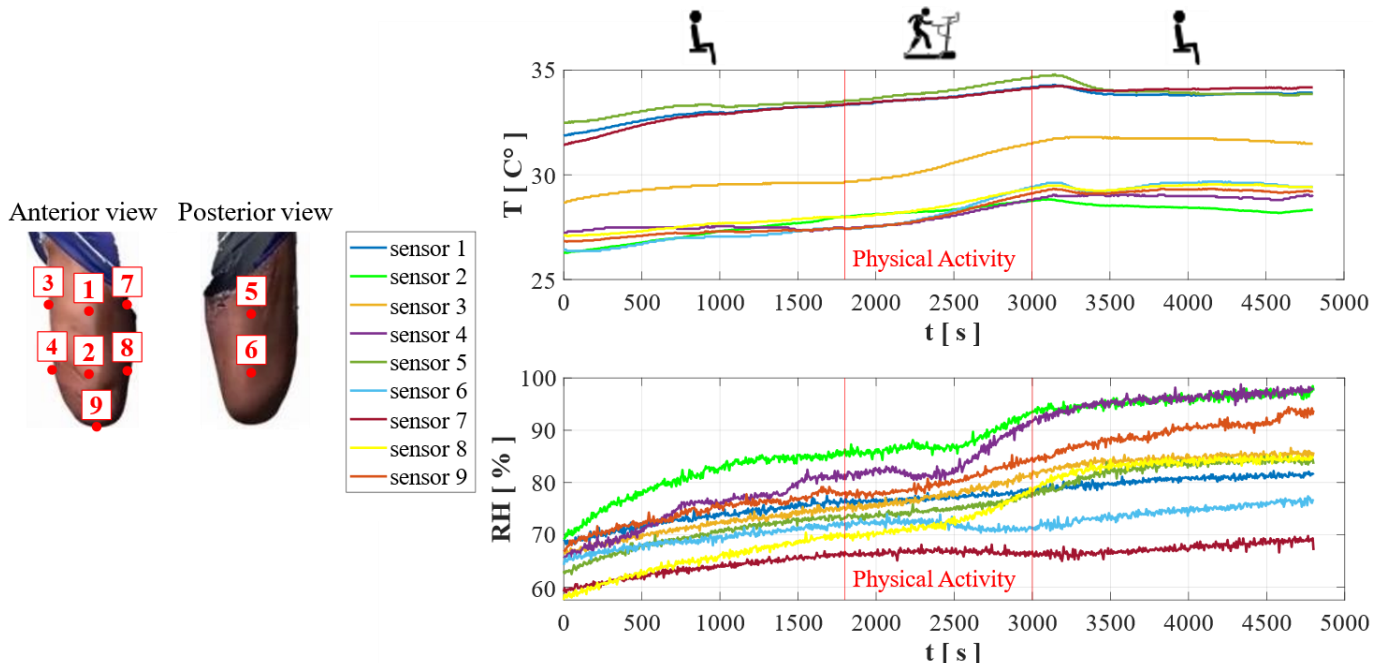

Fig. 13. Temperature and relative humidity values within the soft socket during 30 minutes of resting, 20 minutes of walking at a self-selected speed on a treadmill, and a 30 minutes of seated resting period post-exercise.

The final results are similar to those reported in the previous clinical studies, with higher temperature values in the proximal than the distal region, and relative humidity that increased continuously during the entire test [18]. In particular, the temperature was found slightly lower with respect to the previous works that, however, were carried out only on transtibial amputees. Indeed, in our study, the initial temperature after 30 minutes of resting was equal to 29.8 ± 2.8 °C compared to 31.0 ± 1.5 °C [11] and 32.2 ± 1.3 °C [43] measured respectively in nine and five transtibial amputees. Furthermore, the physical activity caused an increment of 1.3 °C compared to 3.1 °C reported by Klute et al. [11]. The temperature increments are mainly due to the silicone layer of the socket, as already reported in the literature for silicone liners [5], [44]. Indeed, silicone material allows for lowering pressures on tissues and other advantages but features a very low thermal conductivity. Since an increment of 1–2 °C is sufficient to cause discomfort to the participant, additional efforts are still required to improve the thermal conditions of the residual limb within the socket. In this regard, the most widespread solution is based on the exploitation of perforating techniques to create micro-holes able to improve perspiration and sweating expulsion [45]–[48]. However, this approach may affect the vacuum suspension system of the socket. For this reason, it is usually exploited only for transtibial prostheses, or with other suspension systems, e.g., a pin-locking mechanism, which, however, turns out heavy and bulky [46], [47].

The overall comfort of the new socket was evaluated using a modified version of the PEQ and the Socket Comfort Score. The recruited participant expressed a high level of acceptance for the new socket, along with extremely positive feedback. While the tests were carried out with only one participant, these results provide pilot evidence of the potential of the proposed solution. In the future, the recruitment of a statistically significant number of participants will enable a conclusive assessment of its effectiveness and acceptability.

The new socket featured four commercial pre-gelled electrodes and three vibrotactile units at the interface with the residual tissues. Through the electrodes, sEMG signals were acquired to infer the motor intention of the recruited participant by a decoding algorithm based on a Support Vector Machines approach [29]. In the future, promising dry electrode technologies, such as textile-based solutions [49], will be investigated to further improve integration while keeping a comfortable and soft interface. Indeed, in the current design, disposable pre-gelled electrodes can be easily replaced thanks to the mechanical clips. However, they are fragile components that could be frequently damaged. This was also confirmed by the noisy signals acquired through the Bicep Femoris channel (Fig. 10), probably caused by damage to the corresponding electrode. Anyhow, the performed tests showed promising results, with an accuracy in the classification of the performed tasks higher than 73% with all the three analyzed gait cycle sub-windows (i.e., 0% - 100%, 0% - 60%, -30% - 20%) and with both linear and polynomial 2nd order kernels. In particular, the window that considered the EMG signals acquired between 0% and 60% of the gait cycle allowed for the highest median accuracy, equal to 86% for both kernel options, but with a lower IQR value for the polynomial one, which points out an improvement in terms of performance stability (Fig. 11).

The feasibility to equip the prosthetic socket with an augmenting feedback system was assessed through a psychophysical experiment based on delivering vibrotactile stimuli that the participant should identify. The three vibrotactile units were activated randomly and at different stimulation levels (i.e., 2g, 3g and 4g ERM motor peak acceleration). The accuracy was computed and as expected, the results showed increasing accuracy with the increment of the stimulation intensity. The stimuli at 4g acceleration were the best-perceived ones when the participant was sat. Slight differences were found between the intermediate and the highest intensity levels for the standing position, being the former, i.e., 3g, greater than the latter, i.e., 4g. Overall, although the differences between the two postures were not remarkable, perception performance in the sitting position was slightly better (Fig. 12). This result may be attributed to the increased pressure between the stump and the socket inner surface, as well as the deformation of the thigh soft tissues while standing, thus causing altered perception of vibrations. In both the cases, also less strong vibrations have been perceived with an accuracy over the random guess threshold (equal to 33% accuracy).

A thorough insight into the normalized confusion matrices suggested that the accuracy in perceiving singularly activated units was the highest and less misrecognized in both the sitting and the standing positions. Specifically, VT1 and VT2 were correctly identified most of the times, whereas VT3 was sometimes confounded with VT2 or the pair VT2-VT3. This trend was confirmed when considering the activation of VT pairs and triple as well, since classification errors originated from the low ability of the participant to distinguish VT2 from VT3 stimuli. As an example, the activation of all the VTs at the same time was misclassified as the activation of the VT1-VT3 pair in about half the cases, suggesting that the activation of the medial (VT3) and the anterior (VT2) units were often perceived as a single stimulus (Fig. 12). Being these two units placed at a shorter distance than the distance between VT1 and VT2, the obtained results suggested that the participant's two-point discrimination threshold for vibrations on the upper leg is greater than 7.5 cm, against the 4.5 cm distance between two static tactile cues found by Weinsten [50]. In this regard, it is worth considering that amputees usually present an altered and inhomogeneous tactile sensitivity on the residual limb [51]. In addition, discrimination of vibratory cues, unlike that of static stimuli, is somehow affected by the propagation effect of the vibrating waves through the tissues, which also depends on the specific properties of the skin at that site [52].

However, the analysis of the effect of the different stimulation levels on the accuracy to localize stimuli demonstrated that stronger vibrations determined better results, with less sparse confusion matrices. The discrimination ability between VT2 and VT3 activations improved with the intensity increase in the sitting position, whilst VT2 remained highly misrecognized in paired activations while standing (Supplementary Fig.1S). These findings may provide useful information on how designing a feedback pattern able to provide easily interpretable information about the user's gait [53].

In tasks involving motor control and coordination, vision serves as a primary source of feedback [31]. The eyes continuously provide information about the position of body parts, the surrounding environment, and potential obstacles. Thus, future studies could include additional tests with vibrotactile feedback, both with and without the participant's eyes open. This could enable a more comprehensive analysis of the role of vision in sensory feedback and effective sensory-motor integration.

The main limitation of the proposed study is that only one participant was involved due to the need to produce a custom socket for each user. Additionally, some translational challenges have to be overcome to achieve a smart socket that can be really integrated into a robotic prosthesis. The *VibroBoard* used for the vibrotactile stimuli should be miniaturized and the control unit for the motor intention decoding based on sEMG signals should be programmed on-chip. However, the proposed solution is one of the first attempts in the development of a bidirectional interface for transfemoral prostheses based on a non-invasive approach that relies on the integration of smart technologies into the socket. Thus, the proposed solution opens up new possibilities for robotic prostheses, paving the way for the development of an effective bidirectional control of these devices.

REFERENCES

[1] M. Windrich, M. Grimmer, O. Christ, S. Rinderknecht, and P. Beckerle, "Active lower limb prosthetics: a systematic review of design issues and solutions," *Biomed. Eng. OnLine 2016 153*, vol. 15, no. 3, pp. 5–19, Dec. 2016.

[2] J. Mendez, S. Hood, A. Gunnel, and T. Lenzi, "Powered knee and ankle prosthesis with indirect volitional swing control enables level-ground walking and crossing over obstacles," *Sci. Robot.*, vol. 5, no. 44, p. 6635, Jul. 2020.

[3] A. Mazzarini *et al.*, "A low-power ankle-foot prosthesis for push-off enhancement," *Wearable Technol.*, vol. 4, p. e18, 2023.

[4] P. Beckerle, O. Christ, T. Schürmann, J. Vogt, O. von Stryk, and S. Rinderknecht, "A human–machine-centered design method for (powered) lower limb prosthetics," *Rob. Auton. Syst.*, vol. 95, pp. 1–12, Sep. 2017.

[5] L. Paternò, M. Ibrahimi, E. Gruppioni, A. Menciassi, and L. Ricotti, "Sockets for limb prostheses: A review of existing technologies and open challenges," *IEEE Trans. Biomed. Eng.*, vol. 65, no. 9, pp. 1996–2010, Sep. 2018.

[6] R. Safari, "Lower limb prosthetic interfaces: Clinical and technological advancement and potential future direction," *Prosthet. Orthot. Int.*, vol. 44, no. 6, pp. 384–401, Dec. 2020.

[7] H. E. Meulenbelt, J. H. Geertzen, M. F. Jonkman, and P. U. Dijkstra, "Determinants of Skin Problems of the Stump in Lower-Limb Amputees," *Arch. Phys. Med. Rehabil.*, vol. 90, no. 1, pp. 74–81, Jan. 2009.

[8] T. R. Dillingham, L. E. Pezzin, E. J. MacKenzie, and A. R. Burgess, "Use and satisfaction with prosthetic devices among persons with trauma-related amputations: a long-term outcome study," *Am. J. Phys. Med. Rehabil.*, vol. 80, no. 8, pp. 563–571, 2001.

[9] L. Paternò *et al.*, "Residual limb volume fluctuations in transfemoral amputees," *Sci. Rep.*, vol. 11, no. 1, pp. 1–11, Jun. 2021.

[10] L. Paternò *et al.*, "Quantitative analysis of interface pressures in transfemoral prosthetic sockets," *Prosthetics Orthot. Int.*, vol. Publish Ah, pp. 1–8, 2023.

[11] G. K. Klute, E. Huff, and W. R. Ledoux, "Does activity affect residual limb skin temperatures?," *Clin. Orthop. Relat. Res.*, vol. 472, no. 10, pp. 3062–3067, 2014.

[12] B. Chen, Y. Feng, and Q. Wang, "Combining vibrotactile feedback with volitional myoelectric control for robotic transtibial prostheses," *Front. Neurorobot.*, vol. 10, no. AUG, p. 8, 2016.

[13] B. J. Hafner and J. E. Sanders, "Considerations for development of sensing and monitoring tools to facilitate treatment and care of persons with lower limb loss," *J. Rehabil. Res. Dev.*, vol. 51, no. 1, p. 1, 2014.

[14] G. M. Hefferman, F. Zhang, he Huang, and M. J. Nunnery, "Integration of surface electromyographic sensors with the transfemoral amputee socket: A comparison of four differing configurations," *Prosthet. Orthot. Int.*, vol. 39, no. 2, pp. 166–173, Jan. 2015.

[15] WillowWood, "Alpha Control Liner System." [Online]. Available: https://willowwood.com/products-services/liners/upper-extremity/alpha-control-liner-system/. [Accessed: 07-Aug-2023].

[16] K. M. Henrikson, E. J. Weathersby, B. G. Larsen, J. C. Cagle, J. B. McLean, and J. E. Sanders, "An inductive sensing system to measure in-socket residual limb displacements for people using lower-limb prostheses," *Sensors (Switzerland)*, vol. 18, no. 11, 2018.

[17] J. Tabor *et al.*, "Textile-Based Pressure Sensors for Monitoring Prosthetic-Socket Interfaces," *IEEE Sens. J.*, vol. 21, no. 7, pp. 9413–9422, 2021.

[18] L. Paternò, V. Dhokia, A. Menciassi, J. Bilzon, and E. Seminati, "A personalised prosthetic liner with embedded sensor technology: A case study," *Biomed. Eng. Online*, vol. 19, no. 1, pp. 1–20, Sep. 2020.

[19] E. Al-Fakih, N. Arifin, G. Pirouzi, F. R. Mahamd Adikan, H. N. Shasmin, and N. A. Abu Osman, "Optical fiber Bragg grating-instrumented silicone liner for interface pressure measurement within prosthetic sockets of lower-limb amputees," *J. Biomed. Opt.*, vol. 22, no. 08, p. 1, 2017.

[20] M. Zhu, S. Biswas, S. I. Dinulescu, N. Kastor, E. W. Hawkes, and Y. Visell, "Soft, Wearable Robotics and Haptics: Technologies, Trends, and Emerging Applications," *Proc. IEEE*, vol. 110, no. 2, pp. 246–272, Feb. 2022.

[21] S. Fatone and R. Caldwell, "Northwestern University Flexible Subischial Vacuum Socket for persons with transfemoral amputation-Part 1: Description of technique," *Prosthet. Orthot. Int.*, vol. 41, no. 3, pp. 237–245, Jun. 2017.

[22] E. Neumann, J. Wong, and R. Drollinger, "Concepts of Pressure in an Ischial Containment Socket: Measu... : JPO: Journal of Prosthetics and Orthotics," *J. Prosthetics Orthot.*, vol. 17, no. 1, pp. 2–11, 2005.

[23] L. Paterno, C. Quaglia, M. Ibrahimi, E. Gruppioni, L. Ricotti, and A. Menciassi, "A new motor-driven smart prosthetic socket," in *7th National Congress of Bioengineering*, 2021.

[24] I. Vujaklija, D. Farina, and O. C. Aszmann, "New developments in prosthetic arm systems," *Orthop. Res. Rev.*, vol. 8, p. 31, Jul. 2016.

[25] E. Rogers, "Neurally-controlled ankle-foot prosthesis with non-backdrivable transmission for rock climbing augmentation," Massachusetts Institute of Technology, 2019.

[26] F. Barberi *et al.*, "Fast Online Decoding of Motor Tasks with Single sEMG Electrode in Lower Limb Amputees," *Biosyst. Biorobotics*, vol. 22, pp. 110–114, Oct. 2018.

[27] B. Silver-Thorn, T. Current, and B. Kuhse, "Preliminary investigation of residual limb plantarflexion and dorsiflexion muscle activity during treadmill walking for trans-tibial amputees," *Prosthet. Orthot. Int.*, vol. 36, no. 4, pp. 435–442, Dec. 2012.

[28] S. Huang and D. P. Ferris, "Muscle activation patterns during walking from transtibial amputees recorded within the residual limb-prosthetic interface," 2012.

[29] F. Barberi *et al.*, "Early decoding of walking tasks with minimal set of EMG channels.," *J. Neural Eng.*, Mar. 2023.

[30] U. Proske and S. C. Gandevia, "The proprioceptive senses: Their roles in signaling body shape, body position and movement, and muscle force," *Physiol. Rev.*, vol. 92, no. 4, pp. 1651–1697, Oct. 2012.

[31] E. Martini *et al.*, "Increased Symmetry of Lower-Limb Amputees Walking with Concurrent Bilateral Vibrotactile Feedback," *IEEE Trans. Neural Syst. Rehabil. Eng.*, vol. 29, pp. 74–84, 2021.

[32] C. Fanciullacci *et al.*, "Survey of transfemoral amputee experience and priorities for the user-centered design of powered robotic transfemoral prostheses," *J. Neuroeng. Rehabil.*, vol. 18, no. 1, pp. 1–25, Dec. 2021.

[33] M. Asif *et al.*, "Advancements, Trends and Future Prospects of Lower Limb Prosthesis," *IEEE Access*, vol. 9, pp. 85956–85977, 2021.

[34]   A. Khajuria and D. Joshi, "Effects of vibrotactile feedback on postural sway in trans-femoral amputees: A wavelet analysis," *J. Biomech.*, vol. 115, p. 110145, Jan. 2021.

[35]   D. Rusaw, K. Hagberg, L. Nolan, and N. Ramstrand, "Can vibratory feedback be used to improve postural stability in persons with transtibial limb loss?," *J. Rehabil. Res. Dev.*, vol. 49, no. 8, pp. 1239–1253, 2012.

[36]   A. Plauche, D. Villarreal, and R. D. Gregg, "A Haptic Feedback System for Phase-Based Sensory Restoration in Above-Knee Prosthetic Leg Users," *IEEE Trans. Haptics*, vol. 9, no. 3, pp. 421–426, Jul. 2016.

[37]   I. Cesini *et al.*, "Perception of Time-Discrete Haptic Feedback on the Waist is Invariant with Gait Events," *IEEE Trans. Neural Syst. Rehabil. Eng.*, vol. 28, no. 7, pp. 1595–1604, Jul. 2020.

[38]   Maxim Integrated, "DS1923 iButton Hygrochron Temperature/Humidity Logger with 8KB Datalog Memory Absolute Maximum Ratings Electrical Characteristics," 2015. [Online]. Available: www.maximintegrated.com. [Accessed: 14-Jun-2022].

[39]   R. S. Hanspal, K. Fisher, and R. Nieveen, "Prosthetic socket fit comfort score.," *Disabil. Rehabil.*, vol. 25, no. 22, pp. 1278–1280, 2003.

[40]   C. McCloskey, J. Kenia, F. Shofer, J. Marschalek, and T. R. Dillingham, "Improved Self-Reported Comfort, Stability, and Limb Temperature Regulation With an Immediate Fit, Adjustable Transtibial Prosthesis," *Arch. Rehabil. Res. Clin. Transl.*, vol. 2, no. 4, p. 100090, Dec. 2020.

[41]   M. W. Legro, G. D. Reiber, D. G. Smith, M. Del Aguila, J. Larsen, and D. Boone, "Prosthesis evaluation questionnaire for persons with lower limb amputations: Assessing prosthesis-related quality of life," *Arch. Phys. Med. Rehabil.*, vol. 79, no. 8, pp. 931–938, Aug. 1998.

[42]   J. E. Sanders *et al.*, "A motor-driven adjustable prosthetic socket operated using a mobile phone app: A technical note," *Med. Eng. Phys.*, vol. 68, pp. 94–100, 2019.

[43]   J. T. Peery, W. R. Ledoux, and G. K. Klute, "Residual-limb skin temperature in transtibial sockets," *J. Rehabil. Res. Dev.*, vol. 42, no. 2, pp. 147–154, Mar. 2005.

[44]   R. J. Williams, E. D. Washington, M. Miodownik, and C. Holloway, "The effect of liner design and materials selection on prosthesis interface heat dissipation," *Prosthet. Orthot. Int.*, vol. 42, no. 3, pp. 275–279, Jun. 2018.

[45]   R. Caldwell and S. Fatone, "Technique for Perforating a Prosthetic Liner to Expel Sweat," *J. Prosthetics Orthot.*, vol. 29, no. 3, pp. 145–147, Jul. 2017.

[46]   Blatchford, "Silcare Silicone Liners from Endolite." [Online]. Available: http://www.silcareliners.com/us/. [Accessed: 08-Aug-2023].

[47]   Uniprox, "SoftskinAir." [Online]. Available: https://www.softskinair.com/#ad500. [Accessed: 08-Aug-2023].

[48]   M. McGrath, J. McCarthy, A. Gallego, A. Kercher, S. Zahedi, and D. Moser, "The influence of perforated prosthetic liners on residual limb wound healing: a case report," *Can. Prosthetics Orthot. J.*, Aug. 2019.

[49]   "Systematic review of textile-based electrodes for long-term and continuous surface electromyography recording."

[50]   S. Weinstein, "Intensive and extensive aspects of tactile sensitivity as a function of body part, sex and laterality," in *First International Symposium on Skin Senses*, 1968, pp. 195–222.

[51]   C. A. Templeton, N. D. J. Strzalkowski, P. Galvin, and L. R. Bent, "Cutaneous sensitivity in unilateral trans-tibial amputees," *PLoS One*, vol. 13, no. 6, p. e0197557, Jun. 2018.

[52]   R. W. Cholewiak and A. A. Collins, "Vibrotactile localization on the arm: Effects of place, space, and age," *Percept. Psychophys.*, vol. 65, no. 7, pp. 1058–1077, 2003.

[53]   S. Choi and K. J. Kuchenbecker, "Vibrotactile display: Perception, technology, and applications," *Proceedings of the IEEE*, vol. 101, no. 9. Institute of Electrical and Electronics Engineers Inc., pp. 2093–2104, 2013.